AGU PUBLICATIONS

Geophysical Research Letters

RESEARCH LETTER
10.1002/2015GL063732

L. Schmid and F. Koch contributed equally.

Key Points:
- Nondestructive snow measurement below snow cover without external information
- Determining snowpack properties by combining radar and low-cost GPS
- Continuous data on liquid water content, snow height, and snow water equivalent

Correspondence to:
L. Schmid and F. Koch,
schmidl@slf.ch;
franziska.koch@lmu.de

Citation:
Schmid, L., F. Koch, A. Heilig, M. Prasch, O. Eisen, W. Mauser, and J. Schweizer (2015), A novel sensor combination (upGPR-GPS) to continuously and nondestructively derive snow cover properties, *Geophys. Res. Lett.*, *42*, doi:10.1002/2015GL063732.

Received 3 MAR 2015
Accepted 5 APR 2015
Accepted article online 8 APR 2015

A novel sensor combination (upGPR-GPS) to continuously and nondestructively derive snow cover properties

Lino Schmid[1], Franziska Koch[2], Achim Heilig[3], Monika Prasch[2], Olaf Eisen[3,4], Wolfram Mauser[2], and Jürg Schweizer[1]

[1]WSL Institute for Snow and Avalanche Research SLF, Davos Dorf, Switzerland, [2]Department of Geography, Ludwig-Maximilians-Universität München, Munich, Germany, [3]Institute of Environmental Physics, University of Heidelberg, Heidelberg, Germany, [4]Alfred-Wegener-Institut Helmholtz Zentrum für Polar- und Meeresforschung, Bremerhaven and Universität Bremen, Bremen, Germany

Abstract Monitoring seasonal snow cover properties is critical for properly managing natural hazards such as snow avalanches or snowmelt floods. However, measurements often cannot be conducted in difficult terrain or lack the high temporal resolution needed to account for rapid changes in the snowpack, e.g., liquid water content (LWC). To monitor essential snowpack properties, we installed an upward looking ground-penetrating radar (upGPR) and a low-cost GPS system below the snow cover and observed in parallel its evolution during two winter seasons. Applying external snow height (HS) information, both systems provided consistent LWC estimates in snow, based on independent approaches, namely measurements of travel time and attenuation of electromagnetic waves. By combining upGPR and GPS, we now obtain a self-contained approach instead of having to rely on external information such as HS. This allows for the first time determining LWC, HS, and snow water equivalent (SWE) nondestructively and continuously potentially also in avalanche-prone slopes.

1. Introduction

The snow cover is not only an important component of the climate system [*Vaughan et al.*, 2013] and a vital reservoir of freshwater but also can contribute to natural disasters such as floods and snow avalanches. For hazard mitigation, continuous information on snow height (HS), snow water equivalent (SWE), and liquid water content (LWC) of snow are highly demanded. HS and SWE are important parameters describing the total amount of snow. The evolution of LWC, or the wetness of the snowpack, is an indicator for snowmelt and snow stability. Melting at the snow surface affects the albedo that is a very important parameter for modeling the climate system. The temporal evolution of these snow cover properties is essential for, e.g., snow avalanche [*Baggi and Schweizer*, 2009; *Mitterer et al.*, 2011a] or flood forecasts [*Bacchi and Ranzi*, 2003; *Jasper et al.*, 2002]. In situ snowpack and meteorology observations are highly demanded input variables for snowpack modeling [*Bartelt and Lehning*, 2002; *Brun et al.*, 1992, 1989; *Lehning et al.*, 2002a, 2002b] as well as global climate simulations [*Barnett et al.*, 2005; *Lemke et al.*, 2007; *Loth et al.*, 1993] and hydrological models and water use applications [*Koch et al.*, 2011; *Martinec and Rango*, 1986; *Mauser and Bach*, 2009; *Prasch et al.*, 2013; *Strasser and Mauser*, 2001; *Warscher et al.*, 2013].

Several satellite and ground-based measurements exist to monitor snow properties but are often difficult to apply in high mountain regions and particularly when the snow becomes wet. This is especially the case for avalanche-prone slopes, where up to date, it is impossible to continuously and nondestructively measure HS, SWE, and LWC. Current remote sensing techniques apply visible and infrared as well as active and passive microwaves, in particular to monitor changes over large areas in the polar regions (e.g., tundra and sea ice) [e.g., *Bartsch et al.*, 2007; *Dozier and Painter*, 2004; *Frei et al.*, 2012; *Langlois et al.*, 2007; *Pulliainen and Hallikainen*, 2001; *Shi et al.*, 1994; *Stiles and Ulaby*, 1980; *Tedesco et al.*, 2013]. However, their applicability is inappropriate for steep slopes in mountainous terrain due to layover and foreshortening effects. Moreover, their temporal or spatial resolution inhibits reliable monitoring of rapid changes in, e.g., LWC in the snow cover. Ground-based measurements are scarce and often not applicable in complex and remote terrain. Though laser or ultrasonic sensors measure HS continuously, they need to be installed on poles which can easily be destroyed in steep slopes due to snow movements or avalanches. Snow pillows or snow scales

can provide SWE but are only applicable in level terrain. Furthermore, these measurement systems are susceptible to bridging effects and therefore, erroneous measurements may occur, particularly when the snow changes from dry to wet [*Johnson and Marks*, 2004]. Studies exploiting the Global Navigation Satellite System (GNSS) raw data, such as Global Positioning System (GPS) reflectometry, have demonstrated that HS or SWE can be continuously monitored but are presently also limited to flat terrain and are installed on poles [*Jacobson*, 2010; *Larson et al.*, 2009; *McCreight et al.*, 2014; *Najibi and Jin*, 2013; *Ozeki and Heki*, 2012]. Measurements of LWC with dielectric probes like the Denoth sensor [*Denoth*, 1994] or the Finnish Snow Fork [*Sihvola and Tiuri*, 1986] have in common that they are destructive, labor intense, error prone, and miss the subdaily temporal dynamics of melt and refreeze processes. Moreover, due to safety concerns, they are, as well as other manual observations (e.g., following *Fierz et al.* [2009]), not applicable in avalanche-prone terrain.

Two promising methods for continuously and nondestructively measuring snow properties, which are also potentially applicable in complex terrain, are (1) radar systems like an upward looking ground-penetrating radar (upGPR) [*Heilig et al.*, 2010; *Mitterer et al.*, 2011b; *Schmid et al.*, 2014] or an upward looking frequency modulated continuous-wave radar [*Gubler and Hiller*, 1984; *Okorn et al.*, 2014] and (2) a system of small and easy to apply low-cost GPS receivers [*Koch et al.*, 2014]. For this study, we made use of an upGPR and compared and combined the measurements with a GPS system. Both systems are buried underneath the snowpack, continuously record its properties, and work in a similar frequency range, namely the microwave L band. They rely on independent methods: upGPR on velocity and GPS on signal attenuation of the electromagnetic waves [*Bradford et al.*, 2009]. Combined with external HS information, these two methods are among the first systems that can reliably determine bulk LWC of snow nondestructively [*Koch et al.*, 2014; *Schmid et al.*, 2014].

The aim of this study is to compare the LWC derivations of both systems and to combine the two methods (upGPR and GPS) in order to continuously and nondestructively derive—with this novel sensor combination—the essential snow properties LWC, HS, and SWE, even without additional external information and also during wet snow conditions.

2. Methods

2.1. Weissfluhjoch Study Site and Accompanying Data

The upGPR [*Schmid et al.*, 2014] and GPS [*Koch et al.*, 2014] measurements were performed at the flat study site Weissfluhjoch (Davos, Switzerland) at 2540 m asl. Meteorological and snow cover properties are recorded with numerous sensors [*Marty and Meister*, 2012; *Mitterer et al.*, 2011b]. We made use of a laser gauge and two ultrasonic sensors to measure HS and a snow scale and a snow pillow to measure SWE. Manual snow profiles, in accordance to *Fierz et al.* [2009], were performed on a biweekly basis within 2–8 m of the location where the upGPR was buried [*Schmid et al.*, 2014]. In addition to the conventional snow profile, we recorded LWC using a capacity probe [*Denoth*, 1994] and during the winter season 2012–2013, also the Finnish Snow Fork [*Sihvola and Tiuri*, 1986]. SWE was determined by measuring snow density in the pit multiplied by HS. Furthermore, HS was directly measured above the upGPR by using an avalanche probe. The height of new snow (HN) accumulated during a standard observing period of 24 h was measured every morning at approximately 8 A.M. as described in *Fierz et al.* [2009]. The location of the upGPR, the GPS antennas, the profile line, the other measuring devices used in this study as well as the distances between the sensors are shown in Figure 1.

2.2. upGPR

The radar instrumentation as well as the radar data processing is described in *Schmid et al.* [2014]. In this study, we made use of the 1.6 GHz data set. We determined the two-way travel time of the snow surface reflection using the semiautomated picking algorithm [*Schmid et al.*, 2014, p. 512]. HS was calculated according to *Schmid et al.* [2014, equation (1)] assuming a constant speed of the electromagnetic wave of 0.23 m ns^{-1} as suggested by *Mitterer et al.* [2011b], which is the speed in dry snow with a density (ρ_d) of 357 kg m^{-3} [*Schmid et al.*, 2014]. HS can only be determined under dry snow conditions. If an external HS measurement is available, the real part of the bulk relative effective dielectric permittivity [*Schmid et al.*, 2014, equation (6)] and the LWC can be derived after *Roth et al.* [1990] with the parameters defined in *Schmid et al.* [2014, equation (5)] assuming a constant value of ρ_d (357 kg m^{-3}).

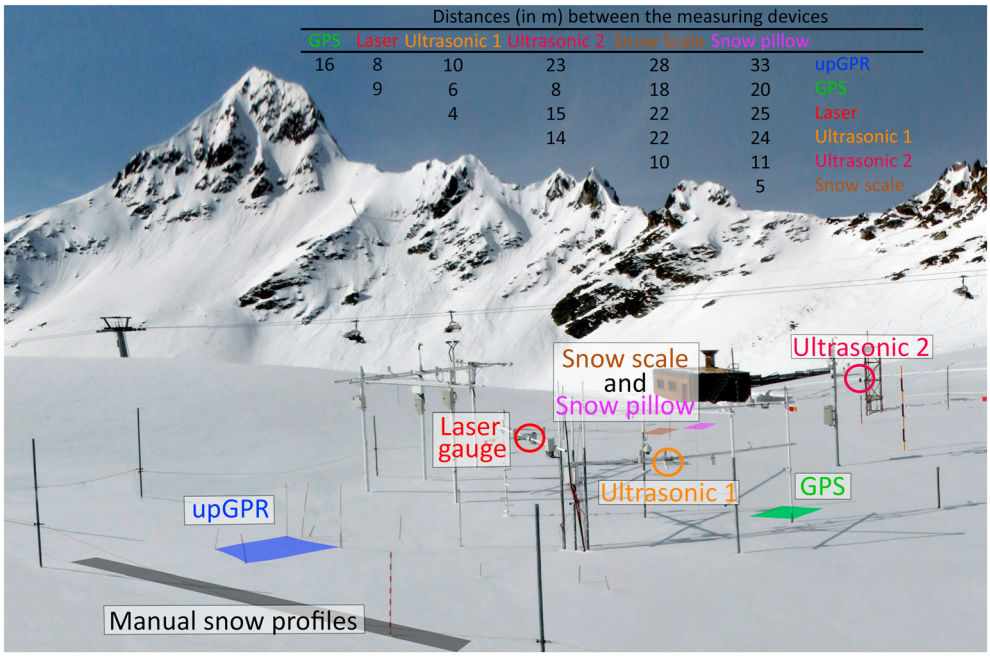

Figure 1. Overview of the study site Weissfluhjoch and the location of the measurement instruments and the profile line. The upGPR and the two GPS antennas as well as the snow scale and the snow pillow are buried in the ground below the snow cover. Ultrasonic 1 and 2 and the laser gauge are mounted on poles above the snow cover. The distances between the measuring devices are shown at the top.

2.3. GPS

The nondestructive low-cost GPS measurement setup and the GPS data processing are described in *Koch et al.* [2014]. For redundancy, two GPS antennas were buried underneath the snowpack. The freely available GPS L1 band information is transmitted at a frequency of 1.57542 GHz. The calculation of LWC is based on GPS signal strength losses in snow. The LWC model described in *Koch et al.* [2014] considers attenuation, reflection, and refraction processes at the snow surface and within the snowpack and requires an external HS measurement as well as the same assumption for dry snow density ($\rho_d = 357\,\mathrm{kg\,m^{-3}}$). Whereas *Koch et al.* [2014] only considered the mean elevation angle, we now calculated the reflection and refraction for each single elevation angle. Furthermore, to be independent of an above-ground installation, we only used GPS receivers beneath the snow cover for this study, as atmospheric influences are negligible for calculating LWC. LWC is per definition zero for dry snow conditions. However, the values derived from the GPS measurements showed a slight offset, possibly due to elusive further losses by multiple reflections. Because we knew from the upGPR measurements the date of the first wetting of the snowpack [*Schmid et al.*, 2014, p. 514] and hence the duration of the dry snow period, we compensated the offset such that the GPS-derived values of LWC were zero on average during dry snow conditions. For the calculation of the attenuation and reflection processes [*Koch et al.*, 2014, equations (6)–(12)], we considered the complex permittivity of snow. To be consistent with the radar measurements, the real part was also calculated after *Roth et al.* [1990] and the imaginary part after *Tiuri et al.* [1984] [*Koch et al.*, 2014, equations (16) and (17)]. The values of LWC derived separately from the two GPS antennas underneath the snowpack agreed very well as indicated by a root-mean-square deviation (RMSD) of 0.2 percentage points (pp). In the following, the mean of these two recordings will be used.

2.4. Combination of Both Methods

With both systems, operating in the microwave L band, the bulk volumetric LWC can be determined from beneath the snowpack—based on two independent physical approaches applying two-way reflectometry for the upGPR [*Schmid et al.*, 2014] and signal attenuation for the GPS [*Koch et al.*, 2014]. However, both systems required external information on HS and ρ_d to derive LWC. Basically, the following equation with three unknowns had to be solved by both systems:

$$\mathrm{LWC} = f(\mathrm{HS},\ \rho_d). \tag{1}$$

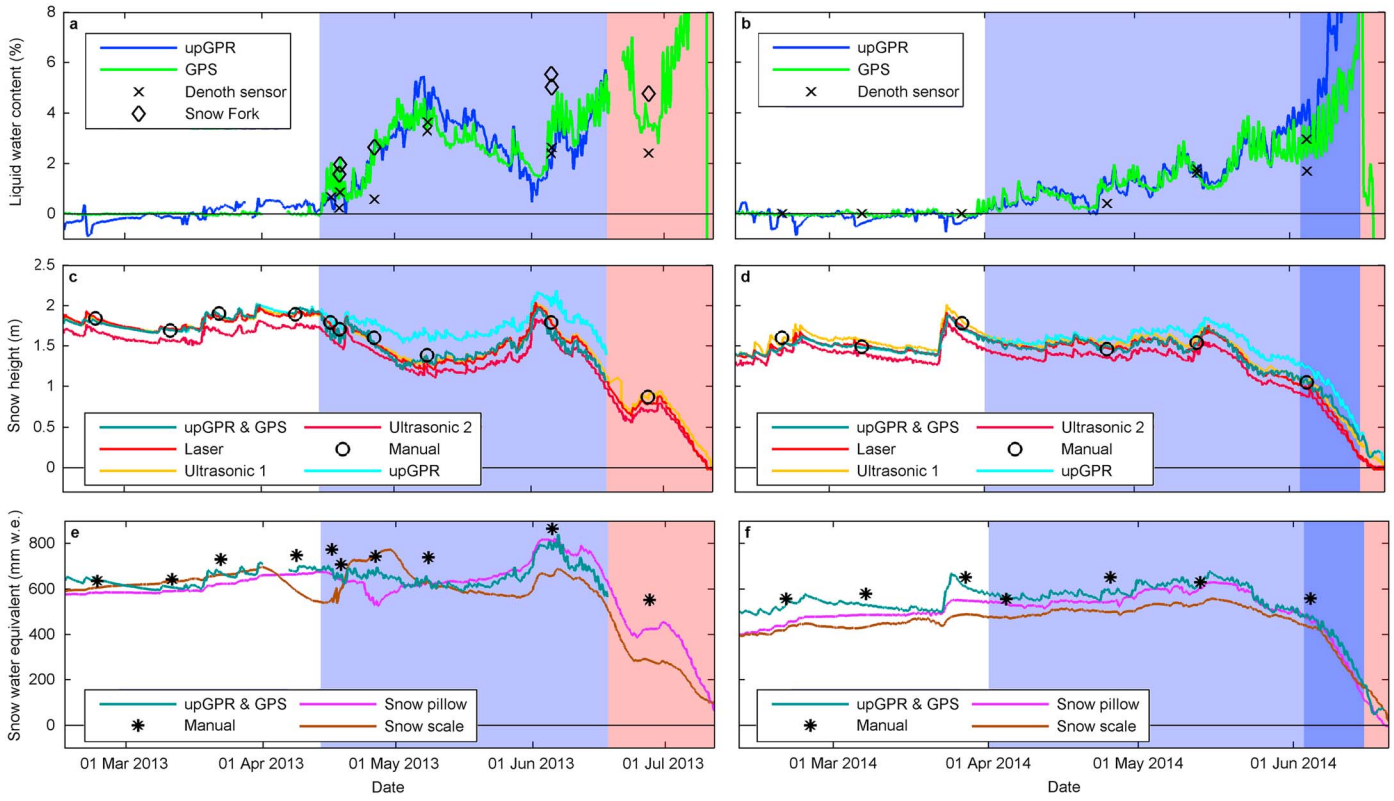

Figure 2. Comparison of snow properties derived from upGPR and GPS with conventional measurements for the time periods 15 February to 12 July 2013 and 10 February to 20 June 2014. The colored backgrounds illustrate in white dry snow and in blue wet snow conditions. Light blue shows when snow height was at least 1 m; dark blue when it was below 1 m. Red backgrounds indicate when there were no upGPR data in 2013 and when the GPS receivers were no longer covered with snow in 2014. (a, b) Bulk volumetric liquid water content derived separately with upGPR and GPS using externally measured snow height data (laser). The markers show the average liquid water content of the snowpack measured in a snow pit with the Denoth sensor and the Snow Fork. (c, d) Snow height derived with the combination of upGPR and GPS, conventionally measured snow height at three different locations as well as manually measured snow height by probing directly above the upGPR. In addition, the snow height measured with the upGPR as described in *Schmid et al.* [2014] without GPS or external information is shown. (e, f) Snow water equivalent derived with the combination of upGPR and GPS, compared with the snow pillow, the snow scale, and manual measurements in a snow pit.

As mentioned above, a constant value for ρ_d (= 357 kg m^{-3}) can be assumed. By combining the two methods, upGPR and GPS, we obtained two equations with two unknowns; and thus, the equations can be solved and HS and LWC can be derived. Knowing ρ_d, HS, and LWC, we can also determine SWE:

$$\mathrm{SWE} = (\rho_d + a\,\mathrm{LWC}\,\rho_w)\,\mathrm{HS}, \tag{2}$$

with ρ_w the density of water and $a = 3.08$ as proposed in *Schmid et al.* [2014].

3. Results

3.1. Comparison of Both Methods

For the winter seasons 2012–2013 and 2013–2014, the bulk volumetric LWC was derived separately from the upGPR and GPS data relying on additional external HS data of a nearby laser sensor. Figures 2a and 2b show the temporal evolution of LWC during the two winter seasons covering dry and wet snow conditions. After 14 April 2013 and 1 April 2014, the snow considerably changed from dry to wet. At 17 June 2013, both systems stopped due to a power failure at the study site; after 19 June 2013, only data from the GPS were available. During wet snow conditions and with a snow height of at least 1 m, the two values of LWC (and their temporal evolution) derived separately from upGPR and GPS data agreed very well as indicated by a RMSD of 0.4 to 0.7 pp (Table 1). However, at the end of the snow-covered period, as HS decreased below 1 m and became more variable due to fast melting, the curves started to deviate. Comparing the LWC values obtained with the Denoth sensor and the Snow Fork with those from upGPR and GPS, resulted in a

Table 1. Root-Mean-Square Deviations for Bulk Volumetric Liquid Water Content ($RMSD_{LWC}$), Snow Height ($RMSD_{HS}$), and Snow Water Equivalent ($RMSD_{SWE}$) for the Seasons 2012–2013 (Above Diagonal, Regular) and 2013–2014 (Below Diagonal, Italic)[a]

		$RMSD_{LWC}$ (pp)			
		upGPR	GPS	Denoth Sensor	Snow Fork
	upGPR	-	**0.7**	0.9	2.2
	GPS	***0.4***	-	0.9	1.5
	Denoth sensor	*0.4*	*0.3*	-	2.1

	$RMSD_{HS}$ (cm)					
	upGPR	upGPR and GPS	Laser	Ultrasonic 1	Ultrasonic 2	Manual
upGPR	-	27.6	26.8	24.5	39.0	18.4
upGPR and GPS	*14.0*	-	**6.6**	7.1	13.7	11.7
Laser	*14.8*	***3.3***	-	3.3	13.8	5.8
Ultrasonic 1	*10.4*	*5.3*	*5.2*	-	15.3	4.8
Ultrasonic 2	*26.1*	*13.5*	*12.6*	*17.3*	-	18.1
Manual	*12.8*	*3.1*	*1.0*	*6.4*	*11.1*	-

	$RMSD_{SWE}$ (mm w.e.)			
	upGPR and GPS	Snow pillow	Snow scale	Manual
upGPR and GPS	-	48	77	82
Snow pillow	*31*	-	112	121
Snow scale	*83*	*55*	-	149
Manual	*43*	*65*	*114*	-

[a]Important results are shown in bold.

RMSD for the Denoth sensor between 0.3 and 0.9 pp and for the Snow Fork between 1.5 and 2.2 pp. The agreement between the two dielectric devices was weak with 2.1 pp.

Diurnal variations of LWC derived separately from upGPR and GPS are shown in Figure 3, exemplarily for late spring 2013. During periods of fair weather and hence melting, the daily fluctuations were prominent but did

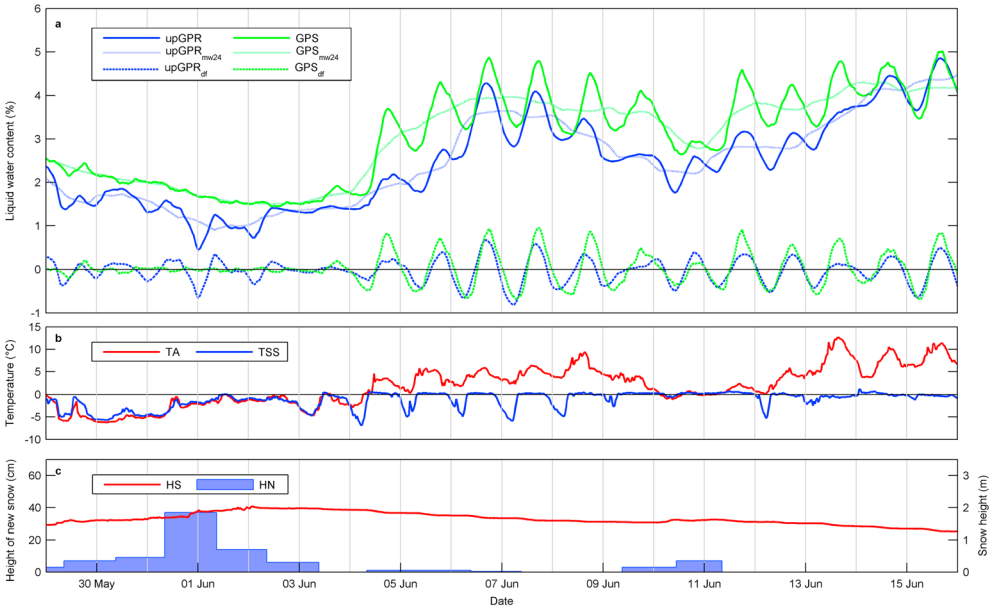

Figure 3. Diurnal variations of the bulk volumetric liquid water content in comparison with temperature and snow height data, exemplarily shown for the time period 29 May to 16 June 2013. (a) Evolution of the liquid water content in snow with daily fluctuations (upGPR and GPS), low-pass filtered with a moving average over 24 h without daily fluctuations ($upGPR_{mw24}$ and GPS_{mw24}), and the difference of liquid water content and the low-pass filtered trend representing the daily fluctuations ($upGPR_{df}$ and GPS_{df}). (b) Air temperature (TA) and snow surface temperature (TSS). (c) Snow height (HS) measured with the laser sensor and height of new snow (HN) as manually measured daily at 8 A.M.

not exceed 2%. When the air temperature was below 0°C or during snowfall (e.g., 29 May to 3 June), the variations were clearly less pronounced. Even though the absolute values of LWC derived from upGPR and GPS differed slightly, the temporal agreement with regard to daily melt and refreeze processes was high.

3.2. Combination of Both Methods

Combining the upGPR and GPS data, HS was derived for the two winter seasons and compared to three conventional and continuous HS measurements (a laser gauge and two ultrasonic sensors) as well as several manual measurements (probing above the upGPR) (Figures 2c and 2d). In addition, HS derived with upGPR as described in *Schmid et al.* [2014] without GPS or external information is shown. In Table 1, the RMSD between all methods is listed for wet snow conditions when HS was at least 1 m. Overall, the correlation between the devices was better in spring 2014 (mean RMSD = 7.9 cm) than in 2013 (mean RMSD = 10 cm). The mean RMSD between the upGPR-GPS combination and the conventional methods was 9.8 cm in spring 2013 (6.5% of the mean HS ($\overline{HS}$) of 150 cm) and 6.3 cm in spring 2014 (4.3% of $\overline{HS}$ of 146 cm). For comparison, the mean RMSD between the conventional methods was 10.2 cm in spring 2013 and 8.9 cm in spring 2014. The RMSD between the upGPR-GPS combination and the laser sensor (which is the nearest sensor to the upGPR and the GPS) was 6.6 cm in 2013 (4.4% of $\overline{HS}$) and 3.3 cm in 2014 (2.3% of $\overline{HS}$). The RMSD between laser and ultrasonic 1 was in a similar range (3.3 cm in 2013 and 5.2 cm in 2014), although they were closer together. Deriving HS from upGPR data only leads to a distinct overestimation during wet snow conditions of on average 27 cm in 2013 and 16 cm in 2014.

Figures 2e and 2f show the SWE derived with the upGPR-GPS combination in comparison with snow pillow and snow scale as well as the manual measurements from the snow pits. Especially in 2013 during the dry-to-wet transition, snow scale and snow pillow deviated considerably. In general, the agreement between the conventional measurements was poorer (mean RMSD of 127 mm w.e. in 2013 and 78 mm w.e. in 2014, Table 1) than compared to the upGPR-GPS combination with a mean RMSD of 69 mm w.e. in 2013 (10.6% of mean SWE ($\overline{SWE}$) of 650 mm w.e.) and 52 mm w.e. in 2014 (9.8% of $\overline{SWE}$ of 532 mm w.e.). Even though the snow pillow is situated furthest away from the upGPR and GPS, the agreement was best in both years.

4. Discussion

4.1. Comparison of Both Methods

We separately derived the bulk volumetric LWC from the upGPR and the GPS data. Both systems recorded data with sensors installed below the snow cover but required externally measured HS and an estimate for ρ_d to derive LWC. The few measurements with the dielectric devices (eight Denoth and five Snow Fork samples in 2013 and three Denoth samples in 2014) revealed values of LWC in a similar range as derived with upGPR and GPS. The RMSD between all measurements and the Snow Fork was quite large with 1.5–2.2 pp; values measured by the Snow Fork were larger than measured by the other methods. This discrepancy was already reported by *Mitterer et al.* [2011b], *Schmid et al.* [2014], and *Techel and Pielmeier* [2011]. In general, the comparison of upGPR and GPS with the dielectric devices is questionable. The latter are destructive, gives only a snap shot in time and is conducted within a snow pit where conditions might change rapidly due to external influences [*Koch et al.*, 2014; *Mitterer et al.*, 2011b; *Schmid et al.*, 2014].

For the first time, it was possible to compare and validate the two methods that both provide bulk LWC in a continuous and nondestructive manner. The comparison between upGPR and GPS showed a high level of agreement with regard to the temporal evolution and the range of LWC values over the entire spring periods 2013 and 2014 (Table 1). Moreover, both systems showed diurnal variations due to melt and refreeze processes—again in good temporal agreement. Differences in LWC between the two methods might occur because HS at the location of the laser sensor differs from HS above the upGPR or the GPS antennas. Considerable differences in LWC between upGPR and GPS were observed only at the end of the snow-covered period (June 2014), when HS decreased below 1 m accompanied with a clear increase in LWC. On the one hand, as the calculation of LWC strongly depends on HS, possible differences in HS between the upGPR and GPS locations and the HS sensor location may be more pronounced shortly before the melt out of the instruments and will have a relatively large effect. In addition, very deep concave furrows of 10 cm were observed on the surface, such that not even the surface was well defined.

On the other hand, the LWC directly upon upGPR and GPS can easily vary due to rapid melting processes within the ripe snowpack (end of June 2013 and beginning of June 2014). Moreover, the formulas applied for the complex permittivity are only valid up to a LWC of approximately 8% [*Lundberg and Thunehed*, 2000; *Mitterer et al.*, 2011b]. However, these deviations were only observed at the very end of the snow-covered season; overall, the agreement between both systems was very good.

4.2. Combination of Both Methods

Combining upGPR and GPS allowed deriving the snow properties LWC, HS, and SWE without using any other external information. As main advantages, this combination is installed below the snow cover and works nondestructively, operates independently from poles and stakes, avoids possible bridging effects within the snow cover, and can therefore potentially be applied in slopes to support avalanche and flood warnings in remote areas. Because the GPS receivers are cheap, the costs of this sensor combination are only negligibly higher than for the upGPR alone. To eliminate a possible error due to spatial variability within the snowpack, especially during melt conditions, both instruments can be installed at the same place at the ground surface, which means that they can observe the same snowpack properties simultaneously.

As illustrated in Figures 2c and 2d, HS derived from the upGPR-GPS combination is in very good agreement with the HS laser measurement during dry and wet snow conditions. Laser, ultrasonic 1, and manual measurements were recorded closest to the upGPR and GPS locations. The RMSD between these measurements and the HS derived from the upGPR-GPS combination are all well below the mean RMSD of all conventional methods. These results suggest that the combined upGPR and GPS approach is suited to determine HS, even during wet snow conditions. Compared to upGPR without external information alone, the RMSD improved from on average 27 cm (2013) and 16 cm (2014) to 9.8 cm and 6.3 cm (Table 1).

Regarding SWE (Figures 2e and 2f), the agreement between snow pillow and snow scale was surprisingly poor despite the fact, that they were situated only 5 m apart from each other. The deviations, especially obvious during the first wetting period in 2013 (1 April–6 May) might be due to bridging effects [*Johnson and Marks*, 2004]. Overall, not being influenced by bridging effects and measuring nondestructively, the SWE and its evolution derived from only upGPR and the combination of upGPR and GPS seemed more reliable. Values of SWE derived from upGPR and GPS were mostly higher than those from snow pillow and snow scale but lower than from manual measurements. These findings can be explained by the observation of increasing HS at the study site from the snow pillow location to the manual snow profiles (Figure 1). The combined approach upGPR and GPS overestimated SWE during and shortly after intense snowfalls, as the bulk density decreased due to the low density of new snow ($\approx$100 kg m^{-3}) (e.g., end of March 2014). Exemplarily for a HS of 1.5 m and a LWC of 4%, an overestimation/underestimation of the bulk density of ±10% leads to an overestimation/underestimation of SWE of ±7%.

5. Conclusions

We derived the bulk volumetric LWC with (1) an upGPR and (2) low-cost GPS receivers buried below the snow cover during two winter seasons. The independently estimated LWC and its evolution agreed very well—suggesting that each of the two methods provides reliable values of LWC. The observation of daily melt-freeze cycles with high temporal resolution may improve runoff calculations within hydrological catchments, which are, e.g., important for hydropower and reservoir management.

We then combined the data from upGPR and GPS to continuously and nondestructively derive LWC, HS, and SWE without the need for additional external information (i.e., HS) from above snow instrumentation; this was not possible before. HS and SWE agreed well with conventional measurements. The novel combination allows to monitor essential snow cover properties from below the snow cover—which potentially can be applied in complex and remote terrain, e.g., in avalanche-prone slopes. We suggest to routinely upgrade all upGPR or other below snowpack techniques with low-cost GPS receivers, as the additional costs and manual effort for the installation are negligible compared with other costs like those of a radar system. The upGPR-GPS combination has the potential to improve avalanche forecasting and flood predictions. It could, moreover, provide an additional proxy for surface melt for comparison with surface energy balance models, which depend on several parameters like albedo. As the combination can estimate SWE with high temporal resolution, our approach may also be suited for large-scale applications, e.g., for catchment-

wide estimation of runoff and hydroelectric power generation potential, as well as provide valuable ground truth data for remote sensing applications, e.g., in the field of glacier and sea ice studies. Therefore, we recommend widespread applications.

Acknowledgments
Lino Schmid was supported by the Swiss National Science Foundation (SNF 200020_144390), Franziska Koch and Achim Heilig by the German Research Foundation (DFG MA 875/12-1 and EI 672/6, respectively). The data presented in this manuscript can be made available on request.

The Editor thanks two anonymous reviewers for their assistance in evaluating this paper.

References

Bacchi, B., and R. Ranzi (2003), Hydrological and meteorological aspects of floods in the Alps: An overview, *Hydrol. Earth Syst. Sci.*, *7*(6), 785–798.
Baggi, S., and J. Schweizer (2009), Characteristics of wet snow avalanche activity: 20 years of observations from a High Alpine Valley (Dischma, Switzerland), *Nat. Hazard.*, *50*, 97–108.
Barnett, T. P., J. C. Adam, and D. P. Lettenmaier (2005), Potential impacts of a warming climate on water availability in snow-dominated regions, *Nature*, *438*, 303–309.
Bartelt, P., and M. Lehning (2002), A physical SNOWPACK model for the Swiss avalanche warning. Part I: Numerical model, *Cold Reg. Sci. Technol.*, *35*(3), 123–145.
Bartsch, A., R. A. Kidd, W. Wagner, and Z. Bartalis (2007), Temporal and spatial variability of the beginning and end of daily spring freeze/thaw cycles derived from scatterometer data, *Remote Sens. Environ.*, *106*, 360–374.
Bradford, J. H., J. T. Harper, and J. Brown (2009), Complex dielectric permittivity measurements from ground-penetrating radar data to estimate snow liquid water content in the pendular regime, *Water Resour. Res.*, *45*, W08403, doi:10.1029/02008WR007341.
Brun, E., E. Martin, V. Simon, C. Gendre, and C. Coleou (1989), An energy and mass model of snow cover suitable for operational avalanche forecasting, *J. Glaciol.*, *35*(12), 333–342.
Brun, E., P. David, M. Sudul, and G. Brunot (1992), A numerical-model to simulate snow-cover stratigraphy for operational avalanche forecasting, *J. Glaciol.*, *38*(128), 13–22.
Denoth, A. (1994), An electronic device for long-term snow wetness recording, *Ann. Glaciol.*, *19*, 104–106.
Dozier, J., and T. H. Painter (2004), Multispectral and hyperspectral remote sensing of alpine snow properties, *Annu. Rev. Earth Planet. Sci.*, *32*(1), 465–494.
Fierz, C., R. L. Armstrong, Y. Durand, P. Etchevers, E. Greene, D. M. McClung, K. Nishimura, P. K. Satyawali, and S. A. Sokratov (2009), *The International Classification for Seasonal Snow on the Ground*, 90 pp., UNESCO-IHP, Paris.
Frei, A., M. Tedesco, S. Lee, J. Foster, D. K. Hall, R. Kelly, and D. A. Robinson (2012), A review of global satellite-derived snow products, *Adv. Space Res.*, *50*, 1007–1029.
Gubler, H., and M. Hiller (1984), The use of microwave FMCW radar in snow and avalanche research, *Cold Reg. Sci. Technol.*, *9*(2), 109–119.
Heilig, A., O. Eisen, and M. Schneebeli (2010), Temporal observations of a seasonal snowpack using upward-looking GPR, *Hydrol. Processes*, *24*, 3133–3145.
Jacobson, M. D. (2010), Inferring snow water equivalent for a snow-covered ground reflector using GPS multipath signals, *Remote Sens.*, *2*, 2426–2441.
Jasper, K., J. Gurtz, and H. Lang (2002), Advanced flood forecasting in Alpine watersheds by coupling meteorological observations and forecasts with a distributed hydrological model, *J. Hydrol.*, *267*(1), 40–52.
Johnson, J. B., and D. Marks (2004), The detection and correction of snow water equivalent pressure sensor errors, *Hydrol. Processes*, *18*(18), 3513–3525.
Koch, F., M. Prasch, H. Bach, W. Mauser, F. Appel, and M. Weber (2011), How will hydroelectric power generation develop under climate change scenarios? A case study in the Upper Danube basin, *Energies*, *4*, 1508–1541.
Koch, F., M. Prasch, L. Schmid, J. Schweizer, and W. Mauser (2014), Measuring snow liquid water content with low-cost GPS receivers, *Sensors*, *14*, 20,975–20,999.
Langlois, A., D. Barber, and B. Hwang (2007), Development of a winter snow water equivalent algorithm using in situ passive microwave radiometry over snow-covered first-year sea ice, *Remote Sens. Environ.*, *106*, 75–88.
Larson, K. M., E. D. Gutmann, V. U. Zavorotny, J. J. Braun, M. W. Williams, and F. G. Nievinski (2009), Can we measure snow depth with GPS receivers?, *Geophys. Res. Lett.*, *36*, L17502, doi:10.1029/2009GL039430.
Lehning, M., P. Bartelt, R. L. Brown, and C. Fierz (2002a), A physical SNOWPACK model for the Swiss avalanche warning. Part III: Meteorological forcing, thin layer formation and evaluation, *Cold Reg. Sci. Technol.*, *35*(3), 169–184.
Lehning, M., P. Bartelt, R. L. Brown, C. Fierz, and P. K. Satyawali (2002b), A physical SNOWPACK model for the Swiss avalanche warning: Part II. Snow microstructure, *Cold Reg. Sci. Technol.*, *35*(3), 147–167.
Lemke, P., J. Ren, R. B. Alley, I. Allison, J. Carrasco, G. Flato, Y. Fujii, G. Kaser, P. Mote, and R. H. Thomas (2007), Observations: Changes in snow, ice and frozen ground, in *Climate Change 2007: The Physical Science Basis; Summary for Policymakers, Technical Summary and Frequently Asked Questions. Part of the Working Group I Contribution to the Fourth Assessment Report of the Intergovernmental Panel on Climate Change*, edited by S. Solomon et al., pp. 337–383, Cambridge Univ. Press, Cambridge, U. K., and New York.
Loth, B., G. Friedrich, and J. M. Oberhuber (1993), A snow cover model for global climatic simulations, *J. Geophys. Res.*, *98*(D6), 10,451–10,464, doi:10.1029/93JD00324.
Lundberg, A., and H. Thunehed (2000), Snow wetness influence on impulse radar snow surveys theoretical and laboratory study, *Nord. Hydrol.*, *31*(2), 89–106.
Martinec, J., and A. Rango (1986), Parameter values for snowmelt runoff modelling, *J. Hydrol.*, *84*(3), 197–219.
Marty, C., and R. Meister (2012), Long-term snow and weather observations at Weissfluhjoch and its relation to other high-altitude observatories in the Alps, *Theor. Appl. Climatol.*, *110*, 573–583.
Mauser, W., and H. Bach (2009), PROMET—Large scale distributed hydrological modelling to study the impact of climate change on the water flows of mountain watersheds, *J. Hydrol.*, *376*, 362–377.
McCreight, J. L., E. E. Small, and K. M. Larson (2014), Snow depth, density, and SWE estimates derived from GPS reflection data: Validation in the western US, *Water Resour. Res.*, *50*, 6892–6909, doi:10.1002/2014WR015561.
Mitterer, C., H. Hirashima, and J. Schweizer (2011a), Wet-snow instabilities: Comparison of measured and modelled liquid water content and snow stratigraphy, *Ann. Glaciol.*, *52*, 201–208.
Mitterer, C., A. Heilig, J. Schweizer, and O. Eisen (2011b), Upward-looking ground-penetrating radar for measuring wet-snow properties, *Cold Reg. Sci. Technol.*, *69*, 129–138.
Najibi, N., and S. Jin (2013), Physical reflectivity and polarization characteristics for snow and ice-covered surfaces interacting with GPS signals, *Remote Sens.*, *5*, 4006–4030.

Okorn, R., G. Brunnhofer, T. Platzer, A. Heilig, L. Schmid, C. Mitterer, J. Schweizer, and O. Eisen (2014), Upward-looking L-band FMCW radar for snow cover monitoring, *Cold Reg. Sci. Technol.*, *103*, 31–40.

Ozeki, M., and K. Heki (2012), GPS snow depth meter with geometry-free linear combinations of carrier phases, *J. Geod.*, *86*, 209–219.

Prasch, M., W. Mauser, and M. Weber (2013), Quantifying present and future glacier melt-water contribution to runoff in a central Himalayan river basin, *Cryosphere*, *7*, 889–904.

Pulliainen, J., and M. Hallikainen (2001), Retrieval of regional snow water equivalent from space-borne passive microwave observations, *Remote Sens. Environ.*, *75*(1), 76–85.

Roth, K., R. Schulin, H. Flühler, and W. Attinger (1990), Calibration of time domain reflectometry for water-content measurement using a composite dielectric approach, *Water Resour. Res.*, *26*(10), 2267–2273, doi:10.1029/WR026i010p02267.

Schmid, L., A. Heilig, C. Mitterer, J. Schweizer, H. Maurer, R. Okorn, and O. Eisen (2014), Continuous snowpack monitoring using upward-looking ground-penetrating radar technology, *J. Glaciol.*, *60*, 509–525.

Shi, J., J. Dozier, and H. Rott (1994), Snow mapping in alpine regions with synthetic aperture radar, *IEEE Trans. Geosci. Remote Sens.*, *32*(1), 152–158.

Sihvola, A., and M. Tiuri (1986), Snow fork for field determination of the density and wetness profiles of a snow pack, *IEEE Trans. Geosci. Remote Sens.*, *24*(5), 717–721.

Stiles, W. H., and F. T. Ulaby (1980), The active and passive microwave response to snow parameters: 1 Wetness, *J. Geophys. Res.*, *85*(C2), 1037–1044, doi:10.1029/JC085iC02p01037.

Strasser, U., and W. Mauser (2001), Modelling the spatial and temporal variations of the water balance for the Weser catchment 1965–1994, *J. Hydrol.*, *254*(1), 199–214.

Techel, F., and C. Pielmeier (2011), Point observations of liquid water content in wet snow-investigating methodical, spatial and temporal aspects, *Cryosphere*, *5*, 405–418.

Tedesco, M., X. Fettweis, T. Mote, J. Wahr, P. Alexander, J. Box, and B. Wouters (2013), Evidence and analysis of 2012 Greenland records from spaceborne observations, a regional climate model and reanalysis data, *Cryosphere*, *7*, 615–630.

Tiuri, M. E., A. H. Sihvola, E. G. Nyfors, and M. T. Hallikainen (1984), The complex dielectric constant of snow at microwave frequencies, *IEEE J. Oceanic Eng.*, *9*(5), 377–382.

Vaughan, D. G., J. C. Comiso, I. Allison, J. Carrasco, G. Kaser, R. Kwok, P. Mote, T. Murray, F. Paul, and J. Ren (2013), Observations: Cryosphere, in *Climate Change 2013: The Physical Science Basis. Contribution of Working Group I to the Fifth Assessment Report of the Intergovernmental Panel on Climate Change*, edited by T. F. Stocker et al., pp. 317–382, Cambridge Univ. Press, Cambridge, U. K., and New York.

Warscher, M., U. Strasser, G. Kraller, T. Marke, H. Franz, and H. Kunstmann (2013), Performance of complex snow cover descriptions in a distributed hydrological model system: A case study for the high Alpine terrain of the Berchtesgaden Alps, *Water Resour. Res.*, *49*, 2619–2637, doi:10.1002/wrcr.20219.